REGISTRATION AND RETRIEVAL OF ELONGATED STRUCTURES IN MEDICAL IMAGES

Alexei Manso Correa Machado and Christiano Augusto Caldas Teixeira

Pontifical Catholic University of Minas Gerais, Av. Dom Jose Gaspar, 500, Belo Horizonte, MG, Brazil

Keywords: Medical imaging, morphology, image registration, information retrieval.

Abstract: This work aims at proposing a set of methods to describe, register and retrieve images of elongated structures from a database based on their shape content. We propose a registration algorithm that jointly takes into account the gross shape of the structure and the shape of its boundary, resulting in anatomically consistent deformations. The method determines a medial axis that represents the full extent of the structure with no branches. Registration follows the linear elasticity model and is implemented through dynamic programming. Discriminative anatomic features are computed from the results of registration and used as variables in a content-based image retrieval system. A case study on the morphology of the corpus callosum in the chromosome 22q11.2 deletion syndrome illustrates the effectiveness of the method and corroborates the hypothesis that retrieval systems may also act as knowledge discovery tools.

1 INTRODUCTION

Elongated structures such as vessels, bones and brain ventricles are of interest in many problems and applications (Toledo et al., 2000; Staal, 2004). Those structures have in common the fact that their gross shape can be efficiently represented by centerlines or medial axes. Contour may present important anatomical features, but the overall shape is, if not more, as important as the shape of the boundary.

This work aims at proposing a set of methods to describe, register and ultimately retrieve images of elongated structures from a database based on their shape content. Image registration techniques have been widely used in morphometry, as it provides detailed description of the anatomy, taking a reference image as a basis for comparison. Registration algorithms are nevertheless computationally costly and, when applied to the whole image or to the boundary of elongated structures, may yield unsatisfactory results. A contribution of this work is a registration algorithm that takes into account both the gross shape of the structure and the shape of its boundary, with emphasis to the former aspect.

Figure 1 shows a schematic of a content-based image retrieval (CBIR) system that follows this approach. A set of images depicting elongated structures is segmented and the structures represented by

their boundaries and medial axes. Another image, taken as a common reference, is deformed through elastic registration so as to align its anatomy with the anatomy of the images in the dataset. The result of registration is a mapping function from each point in the reference to a point in the target image that enable detailed shape description. After the structures have been described, e.g. based on the curvature of their boundaries and medial axes, they are stored in the database for future searching. The querying phase follows the same steps used to convert the images into descriptive features. The query image converted to the corresponding feature vector is compared with the database, the most similar images are retrieved and presented to the user. The user may rank the results according to their relevance, choose one of the retrieved images as a new query or redefine a region of interest that should be given greater priority in the next retrieving iteration. The query vector is therefore updated taking into account the user's feedback.

The characterization of the gross shape is critical to the registration and retrieval of elongated structures. We also present a semi-automatic solution to the extraction of a medial axis that represents the full extent of the structure with no branches. Finally, discriminative anatomic features are computed from the results of registration and used as variables in a CBIR system. A case study on the morphology of the corpus
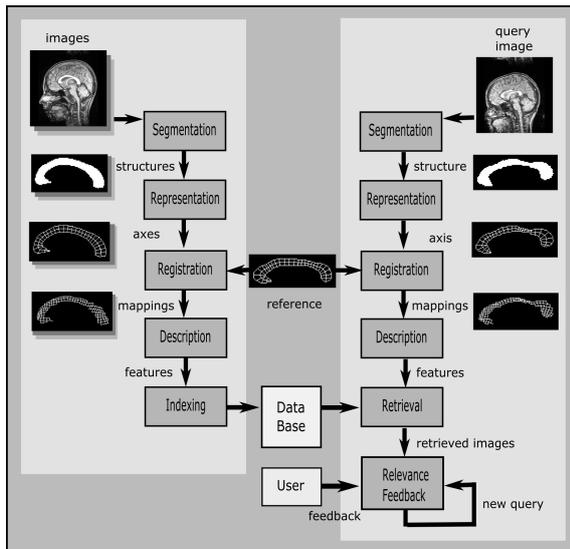
Figure 1: Schematic of a CBIR system based on registration. The left part of the scheme shows the steps performed off-line for each image in the database. The on-line part of the retrieval process is shown in the right. The link between the on-line and off-line phases is the reference image that is registered to the query and to the database, establishing a basis for shape comparison.

callosum in the chromosome 22q11.2 deletion syndrome illustrates the effectiveness of the method and corroborates the hypothesis that CBIR systems may also act as knowledge discovery tools.

2 RELATED WORKS

The representation of elongated structures through single sequences of connected points that describe their intrinsic geometry has been extensively studied. Pioneered by Blum and Nagel (Blum and Nagel, 1978), the use of medial axes to describe 2D shapes is based on the removal of points in the boundary until the gross shape is minimally represented. Many skeleton and thinning algorithms can be found in the literature, revealing the difficulty on determining a standard definition for medial axis (Dvies and Plummer, 1981). Other more complex models include the medial representations (Pizer et al., 2003; Yushkevich et al., 2003), in which the medial axis and a radial scalar field are parametrically described such that the boundary can be further reconstructed, and the medial profiles (Hamarneh et al., 2004), that provide a shape representation and deformation operators that can be used to derive shape distributions.

Registration is considered one of the most important approaches to provide detailed description of shape. Automatic registration algorithms (McInerney

and Terzopoulos, 1996; Toga, 1999) may be applied to the contour (Cootes et al., 1994; Davatzikos and Prince, 1995) or medial axis (Pizer et al., 1996; Golland et al., 1999) of specific structures. Registration is also used together with the medial axis transform (Xie and Heng, 2005) to align the anatomy of structures based on their skeletons.

Retrieval of images based on their content is still in its infancy. Smeulders (Smeulders et al., 2000) and Lew (Lew et al., 2006) present comprehensive discussions on the main aspects and challenges of image retrieval. Muller (Muller et al., 2004) shows how CBIR systems can be used to retrieve images in general medical databases. In the next section, we discuss the specific issues related to the registration and retrieval of images depicting elongated structures and propose a registration algorithm that jointly considers the axis and boundaries of such structures.

3 METHODS

The proposed image retrieval method can be divided into four steps: midline extraction, registration, description and retrieval.

3.1 Midline Extraction

A midline can be defined as a curve that splits the structure into dorsal and ventral regions, such that, at any point, the perpendicular line segments connecting the midline to dorsal and ventral parts of the boundary have roughly the same length (properties of perpendicularity and congruency). Midline extraction starts by determining a skeleton based on a variation of the thinning algorithm described by Gonzalez and Woods (Gonzalez and Woods, 2002), for 8-connected objects. Object points are labeled as 1 and the background is set to 0. In order for the curve to fully extend from one extremity to the other, two object points are manually chosen and forced to be respectively the starting and ending points of the skeleton. Additionally, the thinning algorithm is modified so as to prune any other branches of the structure's skeleton. The final curve is, therefore, a single sequence of pixels, each one connected to two neighbors, with the exception of the starting and ending points.

The following algorithm summarizes skeleton extraction, where p_1 and p_2 are the endpoints; the neighbors of p are denoted as n_i, numbered counterclockwise from 0 (east) to 7 (southeast); function N returns the number of neighbors of p that belong to the object, i.e., $N(p) = \sum_i n_i$; and function S returns the

number of connected sequences of object points in the neighborhood of p, i.e., read as an 8-bit string, the neighbors of p must match the regular expression $0^+1^+0^* \bigcup 1^+0^+1^*$. It can be shown that only 42 neighborhood configurations satisfy the condition to mark a point, so that the algorithm can be efficiently implemented using look-up tables:

Repeat
    For each point p of the object, $p \notin \{p_1, p_2\}$, do
      If $N(p) < 7$ and $S(p) = 1$ and $n_0 n_6 (n_2 + n_4) = 0$
        Mark p to be removed;
    Remove marked points;
    For each point p of the object, $p \notin \{p_1, p_2\}$, do
      If $N(p) < 7$ and $S(p) = 1$ and $n_2 n_4 (n_0 + n_6) = 0$
        Mark p to be removed;
    Remove marked points;
until no more points can be removed.

The linear length of the skeleton is computed considering the distances between each pair of consecutive pixels: pixels connected by a face with distance equals to 1 and the ones connected by a vertex with distance equals to $\sqrt{2}$. The coordinates of the pixels are smoothed and interpolated so as to yield an isotropic rotation-invariant representation of the midline. The derivative of this curve, taken at equidistant points, guides the computation of perpendicular segments that link the dorsal and ventral boundaries of the structure. Problems may occur in regions where the midline presents increased curvature. In this case, it may be impossible to satisfy the requirements of perpendicularity and congruency for the segments. Figure 2 shows an example where two consecutive segments intersect each other as the result of increased midline curvature. A solution for this problem is to violate the property of perpendicularity so that points with increasing coordinates at the midline will be connected to points of non-decreasing coordinates at both boundaries. It is however expected that elongated structures will not frequently incur in this problem.

The curvature (second derivative) of the midline can be determined based on the k-curvature metric, that is defined in each point $p_i = (x_i, y_i)$ as the difference between the average of the derivatives at the k next points and the average of the derivatives at the k previous points (including p_i):

$$kcurv(p_i) = \frac{1}{k}\left(\sum_{j=i+1}^{i+k} d(p_j) - \sum_{j=i-k+1}^{i} d(p_j) \right), \quad (1)$$

$$d(p_j) = \tan^{-1}(x_j - x_{j-1}, y_j - y_{j-1}).$$

Parameter k should be empirically chosen so as to provide enough smoothness. The midline curve should be extrapolated at the extremities (e.g. based on autoregression), so that the curvatures will be computed over all the midline extension. Analogously, the curvature at the dorsal and ventral boundaries should be computed at the intersection of the segments. The curvatures at the midline and boundaries will play a fundamental role as a measure of similarity during registration.
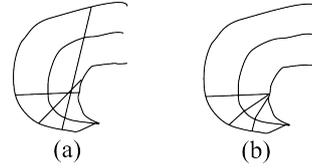
Figure 2: Example where consecutive segments intersect each other as the result of increased midline curvature (a) and the solution to the problem (b).

3.2 Image Registration

The images in the database should be registered to a reference in order to establish a common basis for comparison. Image registration can be stated as the process of determining a correspondence between each point p in the midline of the reference image to a point $u(p)$ in the midline of the subject image. Let $C_M(p) = kcurv(p) - kcurv(u(p))$ be the difference between the k-curvature taken at point p in the reference midline and the k-curvature taken at point $u(p)$ in the subject midline. Analogously, let C_D and C_V be the same difference function computed respectively at the intersection points of the perpendicular segments emanating from the midline with the dorsal and ventral boundaries.

The cost function to be minimized is given as

$$cost = D - S, \quad (2)$$

where D is the deformation penalty and S is the similarity between the curvatures of registered points of the midline, dorsal and ventral boundaries, given as

$$D = \alpha \int_0^1 \left(\frac{du(p)}{dp}\right)^2 dp + \beta \int_0^1 \left(\frac{d^2u(p)}{dp^2}\right)^2 dp,$$

$$S = \sum_{i \in \{M,D,V\}} \gamma_i \int_0^1 C_i(p)^2 dp \quad (3)$$

Parameters α and β weight the amount and smoothness of deformation, respectively. Parameters γ_M, γ_D and γ_V are negative and weight the importance of the similarity terms computed respectively for the midline, dorsal and ventral boundaries.

Registration is performed through dynamic programming, in which equidistant points in the reference midline are mapped to points in the midlines of the database by minimizing the cost function in (2). After registering the midlines and corresponding

boundaries, thin plate splines (Barrodale et al., 1993) are used to interpolate the warping applied to these curves to the whole structure, so that each pixel in the reference image is assigned a displacement vector.

An advantage of the proposed registration algorithm is that it will always map a segment perpendicular to the reference midline to a segment perpendicular to the midline of the subject image. This is a very important constraint to be observed when dealing with elongated structures. Fig 3 shows two examples where an image registration algorithm based only on the boundary or only on the midline would fail to provide satisfactory deformations. The structure in (a) is the reference, whose boundary points *A* and *B* must be found correspondence in the other structures. A registration algorithm that takes into account only the boundaries would map point *A* to *C* (correctly), but *B* to *E* instead of *D*, since the boundary curvature in *B* is more similar to the curvature in *E* than it is in *D*. If, on the other hand, the algorithm is based only on the curvature of the midline, the registration of the reference to the structure in (c) would probably map the segment $\overline{AB}$ to $\overline{HI}$ instead of $\overline{FG}$, ignoring the similarity between the curvatures at the boundaries. The similarity function proposed in (3) avoid both mistakes, since the curvatures at the midline, dorsal and ventral boundaries are jointly taken into account.
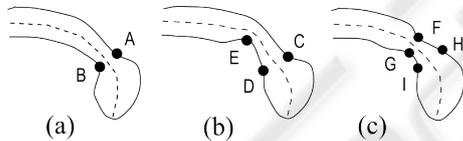
Figure 3: Examples of unsatisfactory registration of the segment $\overline{AB}$ in the reference structure (a) to segment $\overline{CE}$ in (b) and to segment $\overline{HI}$ in (c). An algorithm based on both the boundary and midline would correctly map $\overline{AB}$ to $\overline{CD}$ and $\overline{FG}$.

Evaluating the effectiveness of registration methods is always a difficult task, as ground truth data is usually inexistent, particularly when the structure being registered does not present well-defined landmarks. Alternatively, landmarks may be chosen by experts, but in this case human subjectivity and lack of repeatability should be considered in the analysis. In this work, we designed an interactive interface in which an expert chooses a set of landmarks in the reference structure and the corresponding loci in the subjects. The procedure is repeated after 2 weeks, in order to evaluate repeatability. The results achieved by automatic registration are compared to the mapping provided by the expert: if the result falls within the interval of values provided by the expert, it is considered satisfactory, otherwise the distance in millime-

ters to nearest value is stored and averaged.

3.3 Description

The output of registration is a displacement field that maps each pixel of the reference image to a point in the subject. From this set of vectors, it is possible to obtain diverse measurements that describe the imaged objects, such as point-wise area and length variation, curvature of axes and contours, relationships between axes of orientation, moments and other shape descriptors. Feature selection is a fundamental step in image retrieval systems, as it determines the effectiveness and efficiency of many algorithms. The set of features that will represent the objects should be concise and discriminative, as distinguishing features facilitates the retrieval of relevant images, while non-relevant characteristics are confounders. Feature selection and information retrieval are synergetic steps: while the choice of distinguishing features increases the relevance of retrieval results, retrieval itself act as a "mining" tool, selecting the features that discriminate between classes of images. This is the fundamental relationship that characterizes image retrieval as a potential knowledge discovery methodology. In this work, objects were described as vectors of k-curvatures (1) taken at each matched point of the subjects, after being registered to the reference.

3.4 Image Retrieval

In a CBIR system, the user presents an image as a query, which is registered to the reference image. The features obtained from the resulting mapping function are compared to the features of the images in the database, which have been previously processed and registered to the same reference. Following a measure of similarity, the most similar images are retrieved and presented to the user.

The model used to determine the similarity between two images was the Euclidean distance (Del Bimbo, 1999). If **q** is the feature vector representing the query and $\mathbf{v}_k$ is the feature vector representation of image k in the database, the similarity between them can be computed as

$$sim(\mathbf{v}_k, \mathbf{q}) = ((\mathbf{v}_k - \mathbf{q})^T (\mathbf{v}_k - \mathbf{q}))^{1/2}$$

The performance of an image retrieval system can be evaluated by computing two metrics (Del Bimbo, 1999): The recall of the system is the ability to retrieve relevant images. It is defined as the ratio between the number of retrieved images considered relevant and the total number of relevant images in the database. The precision reflects the ability of the system to retrieve only relevant images. It is defined as

the ratio between the number of retrieved images considered relevant and the total number of retrieved images. The plot of recall × precision gives an estimate of the overall effectiveness of a CBIR system, as a compromise between both performance metrics is expected.

4 EXPERIMENTS

We illustrate the proposed registration-based retrieval system with a case study on the morphology of the corpus callosum in the chromosome 22q11.2 deletion syndrome (DS22q11.2). The DS22q11.2 is an example of genetic abnormality for which many hypotheses on anatomical differences have been recently stated (Machado et al., 2007). This syndrome is the result of a 1.5 - 3Mb microdeletion on the long arm of chromosome 22 and is characterized by a range of medical manifestations that include cardiac, palatal and immune disorders, as well as particular problems in cognitive domains associated with the orienting and executive attention systems and with numerically related processing. Recent studies have drawn particular attention to changes in the corpus callosum — the largest bundle of axons connecting the two hemispheres of the brain, as differences in the shape of this structure may indicate changes in brain connectivity that may be related to the observed cognitive impairments (Simon et al., 2005). We hypothesized that an image retrieval system would be able to retrieve images of subjects sharing the same diagnosis, based on a shape representation of the corpus callosum, if the features used to index the images could be considered discriminative for the syndrome. In this sense, the system would reveal the most distinguishing features associated with the disease.

Participants in this study were 18 children with chromosome 22q11.2 deletion syndrome, ranging in age from 7.3 to 14.0 years (mean,S.D.=9.9,1.4 years) and 18 typically developing control children, ranging in age from 7.5 to 14.2 years (mean,S.D.=10.4,2.0 years) (Simon et al., 2005). Magnetic resonance imaging was performed on a 1.5 Tesla Siemens MAG-NETOM Vision scanner (Siemens Medical Solutions, Erlangen, Germany). For each subject, a high-resolution three-dimensional structural MRI was obtained using a T1-weighted magnetization prepared rapid gradient echo (MP-RAGE) sequence with the following parameters: repetition time (TR) = 9.7 ms, echo time (TE) = 4 ms, flip angle = 12(, number of excitations = 1, matrix size = 256x256, slice thickness = 1.0 mm, 160 sagittal slices, in-plane resolution = 1x1 mm. The midsagittal slice of each brain im-
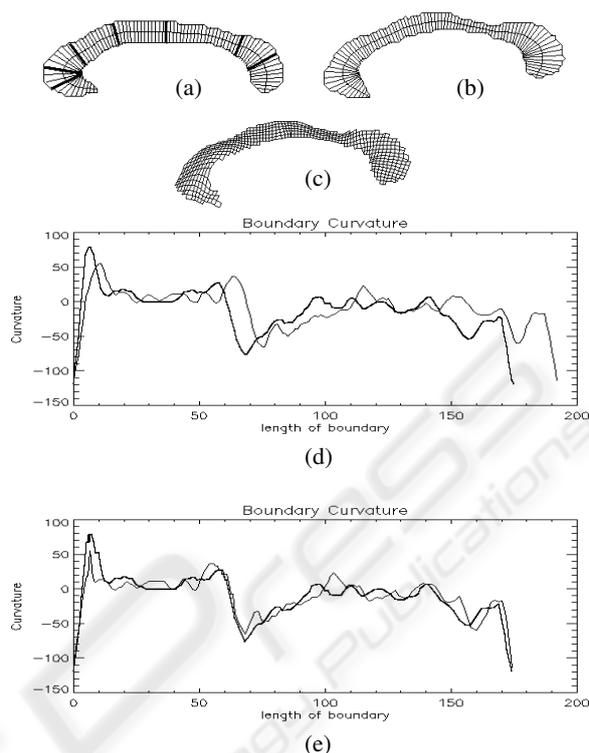
Figure 4: An example of registration. The midline and boundary of the reference (a) is registered to the subject (b) and the result interpolated to the whole structure (c). The original plot of the boundary curvatures (d) and result of registration (e) are also shown, where the curvatures of the template and subject are represented by thick and thin lines, respectively. The 7 landmarks used for registration evaluation, numbered from left to right, are depicted in (a) with thick lines.

age volume was manually extracted as the best plane spanning the interhemispheric fissure, and on which the anterior and posterior commissures and the cerebral aqueduct were visible.

The callosa in the midsagittal images were segmented by manual thresholding and delineation. The boundaries of the callosa were automatically determined using the Rosenfeld algorithm for 8-connected contours (Gonzalez and Woods, 2002). The midlines of the callosa were also extracted based on the algorithm proposed in Section 3.1 and interpolated so as to yield an isotropic rotation-invariant representation, in which any two consecutive sampled points were 1 mm apart. The pointwise curvature of the callosum midline was computed for each subject, using the k-curvature metric (1), where k was empirically chosen to be 10% of the length of the midline, so as to provide enough smoothness.

Shape measurement was performed, by aligning a reference image of the callosum to subject callosa. One of the control subjects was arbitrarily chosen as

the reference. The midline of the reference, sampled at 87 equidistant points, was registered to the subjects' midlines based on the cost function described in (2) with parameters $\alpha=0.001$, $\beta=1000.0$ and $\gamma_i=-1.0$ mm^2/degree^2 for $i \in \{M, D, V\}$, which were empirically determined. The midline curves of the subject callosa were interpolated to provide sub-pixel precision (0.5 mm). The result of registration was a mapping from each of the 87 points in the reference to corresponding points in the subjects. Registration took 7.78 seconds to compute. All methods were implemented in IDL language (Research Systems) and run in a 1.1 GHz Intel Celeron processor computer with 256 MB of RAM, under Windows XP operating system.

Figure 4 shows an example of registration where the reference image described through its midline and perpendicular segments (a) is deformed to match the subject (b). The resulting deformation is shown as a warped grid (c). A plot of the original k-curvatures (in degrees/mm) at the boundaries of both images (in mm), taken counterclockwise from the leftmost endpoint of the midline, is given in (d) and the resulting registration is depicted in (e). The effectiveness of registration was evaluated based on 2 sets of landmarks provided by an expert, taken in an interval of 2 weeks. Seven landmarks were defined at the reference, from anterior to posterior callosum (Figure 4a), and the expert was asked to determine their corresponding loci at each of the 36 subjects. The set of 504 landmarks were compared to the results of registration. Table 1 summarizes the results, where it is possible to compare the average error of the method with the variability of measures provided by the expert, for each landmark. The average error of the method for the whole set of landmarks was 1.7 mm, a satisfactory result considering that the average variability of the expert's measures was 1.2 mm. Larger errors were observed at landmarks 3 and 4 (callosal body) where the subjects present larger variability with respect to curvature. The best results were achieved at landmarks 5 and 6 (posterior callosum) where the errors obtained with automatic registration were smaller than the average variability observed in manual registration.

The results of image retrieval were evaluated with the aid of a simple retrieval environment. Initially, the user browses the database and chooses an image that will represent the query. The system ranks the remaining images, showing the n most relevant to the user appraisal. In this study, we considered as relevant the images that shared the same diagnosis of the query (with or without the deletion). Following the recent findings on anatomic differences in the callo-

sum of these populations (Machado et al., 2007)(see Figure 5), an effective CBIR should be able to retrieve images sharing the same diagnosis, unless outliers would be present in the database.

(a)   (b)
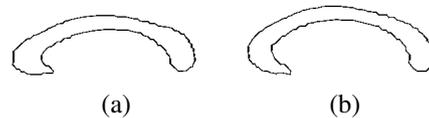
Figure 5: Mean callosal shape for the typically developing children (a) and children with the deletion (b). Controls have shorter, more curved anterior callosum (rostrum and genu) and less curved midbody. Children with the deletion present more arched callosum (larger height/length ratio).

Table 1: Average error (mm) for each landmark, considering manual and automatic registration.

Landmark	0	1	2	3	4	5	6
Manual	0.6	0.4	0.7	1.7	1.3	2.6	1.0
Automatic	1.0	0.9	0.8	3.7	2.4	1.6	0.9

An example of the results of image retrieval is shown in Figure 6. The query image presented by the user (a) is registered to the same reference used in the registration of the images stored in the database. The 10 images that yield greater similarity with respect to the curvature of the midline and boundary are retrieved and displayed (b). Images of controls are shown in gray and images of children with the deletion are shown in black. A plot of the recall $\times$ precision computed after the retrieval of each of the 17 relevant images in the database is presented in (d). In this case, the query is a typical control, yielding high precision.

An example in which an outlier is retrieved is given in Figure 7. The third retrieved image is a control with arched callosum, whereas the query is a child with the deletion. In this case, the precision is affected. Worse result occurs when the query itself is an outlier, as exampled in Figure 8. In this case, the query is a control with longer, less curved rostrum (left-most end of the midline) that is more common in children with the deletion. As a consequence, the precision is drastically affected, staying bellow 50% from the second retrieved image, a level that would be expected by pure chance.

5 CONCLUSIONS

We have addressed the problem of registering and retrieving images of elongated structures. Traditional
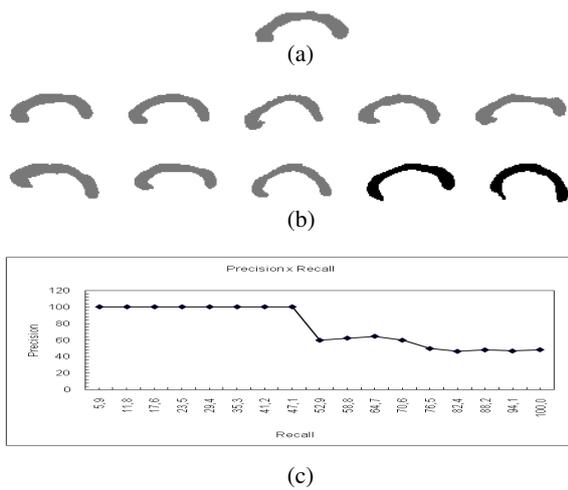
Figure 6: Example of a query image (a) and the result of retrieval (b). The plot of recall × precision is shown in (c).
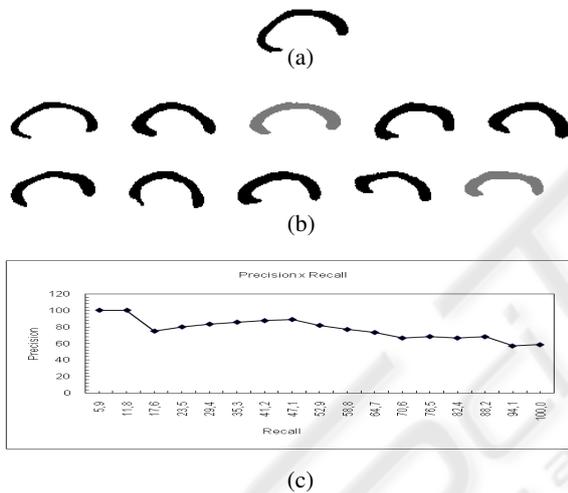
Figure 7: Example of a query image (a) and the result of retrieval (b). In this case, the third best-ranked image is an outlier. The plot of recall × precision is shown in (c).

registration methods may yield anatomically inconsistent results while applying warping models only to the structure's contour or medial axis. The method proposed in this paper jointly registers the medial axis, dorsal and ventral boundaries, avoiding distortions that may impact substantially in the results of further morphometric analyses, hypothesis testing or image retrieval.

The method deserves more systematic evaluation procedures, as visual inspection is subjective and difficult to quantify. A case study on the morphology of the corpus callosum in the 22q11.2 deletion syndrome was used to illustrate the ability of registration to provide effective image retrieval. In the experiments, diagnosis was considered as the ground truth to evalu-
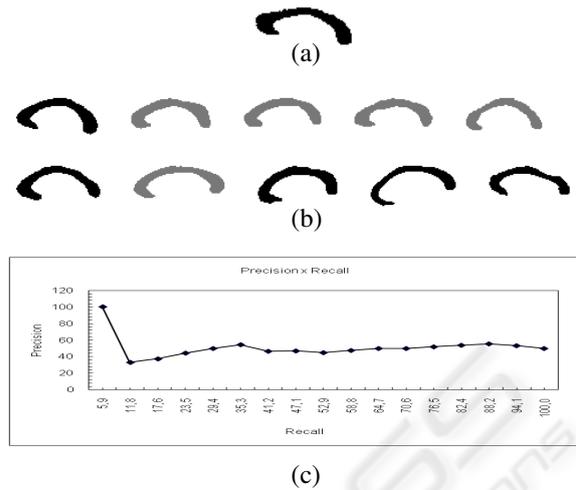
Figure 8: Example of a query image (a) and the result of retrieval (b). In this case, the query is an outlier, yielding poor performance (c).

ate the performance of the retrieval system. Although evidences of shape differences between controls and children with the deletion exist, outliers make evaluation a difficult task. A deficiency of the method is the requirement for manual choice of the midline endpoints, so a fully automated algorithm is already being designed. Another well-known disadvantage of registration-driven retrieval methods is its inadequacy to indexing, limiting the application of these systems to small datasets. Furthermore, the vector model that exhibits excellent performance in text retrieval is not a consensus when dealing with images.

Relevance feedback is an important step that deserves attention. Different similarity functions and query updating models may enhance the effectiveness of image retrieval, as the user's preferences are more rapidly met. Experiments have shown that when the set of features is restricted to specific regions of interest, the precision is enhanced. In the case of the study on the corpus callosum morphometry, restricting the computation of similarity to the anterior-most part of the structure, where the differences between groups are more evident, has increased the number of retrieved images that share the same diagnosis. This ability to cluster images of the same group may qualify image retrieval as a potential knowledge discovery tool. It implements new levels of supporting environments and opens new perspectives to exploratory research in image databases.

ACKNOWLEDGEMENTS

REFERENCES

Barrodale, I., Skea, D., Berkley, M., Kuwahara, R., and Poeckert, R. (1993). Warping digital images using thin plate splines. *Pattern Recognition*, 26(2):375–376.

Blum, H. and Nagel, R. N. (1978). Shape description using weighted symmetric axis features. *Pattern Recognition*, 10(3):167–180.

Cootes, T., Hill, A., Taylor, C. J., and Haslam, J. (1994). Use of active shape models for locating structures in medical images. *Image and Vision Computing*, 12(6):355–365.

Davatzikos, C. and Prince, J. (1995). An active contour model for mapping the cortex. *IEEE Transactions on Medical Imaging*, 14:65–80.

Del Bimbo, A. (1999). *Visual Information Retrieval*. Morgan Kaufman.

Dvies, E. R. and Plummer, A. P. (1981). Thinning algorithms: a critique and a new methodology. *Pattern Recognition*, 14:53–63.

Golland, P., Grimson, W. E. L., and Kikinis, R. (1999). Statistical shape analysis using fixed topology skeletons: Corpus callosum study. *Lecture Notes in Computer Science*, 1613:382–387.

Gonzalez, R. C. and Woods, R. E. (2002). *Digital Image Processing*. Prentice-Hall, Upper Saddle River.

Hamarneh, G., Abu-Gharbieh, R., and McInerney, T. (2004). Medial profiles for modeling deformation and statistical analysis of shape and their use in medical image segmentation. *International Journal of Shape Modeling*, 10(2):187–209.

Lew, M., Sebe, N., Djeraba, C., and Jain, R. (2006). Content-based multimedia information retrieval: State of the art and challenges. *ACM Transactions on Multimedia Computing, Communications, and Applications*, 2(1):1–19.

Machado, A., Simon, T., Nguyen, V., McDonald-McGinn, D., Zackai, E., and Gee, J. (2007). Corpus callosum morphology and ventricular size in chromosome 22q11.2 deletion syndrome. *Brain Research*, 1131:197–210.

McInerney, T. and Terzopoulos, D. (1996). Deformable models in medical image analysis: A survey. *Medical Image Analysis*, 1(2):91–108.

Muller, H., Michoux, N., Bandon, D., and Geissbuhler, A. (2004). A review of content-based image retrieval systems in medical applications-clinical benefits and future directions. *International Journal of Medical Informatics*, 73(1):1–23.

Pizer, S. M., Fletcher, P. T., Joshi, S., Thall, A., Chen, J. Z., Fritsch, D. S., Gash, A. G., Glotzer, J. M., Jiroutek, M. R., Lu, C., Muller, K. E., Tracton, G., Yushkevich, and Chaney, E. (2003). Deformable m-reps for 3D medical image segmentation. *International Journal of Computer Vision*, 55(2):85–106.

Pizer, S. M., Fritsch, D. S., Yushkevich, P., Johnson, V., and Chaney, E. (1996). Segmentation, registration and measurement of shape variation via image object shape. *IEEE Transactions on Medical Imaging*, 18(10):851–865.

Simon, T. J., Ding, L., Bish, J. P., McDonald-McGinn, D. M., Zackai, E. H., and Gee, J. C. (2005). Volumetric, connective, and morphologic changes in the brains of children with chromosome 22q11.2 deletion syndrome: an integrative study. *Neuroimage*, 25:169–180.

Smeulders, A., Worring, M., Santini, S., Gupta, A., and Jain, R. (2000). Content-based image retrieval at the end of the early years. *IEEE Transactions on Pattern Analysis and Machine Intelligence*, 22(12):1349–1380.

Staal, J. (2004). *Segmentation of elongated structures in medical imaging*. PrintPartners Ipskamp, Enschede.

Toga, A. W. (1999). *Brain Warping*. Academic Press, New York.

Toledo, R., Orriols, X., Binefa, X., Radeva, P., Vitria, J., and Villanueva, J. (2000). Tracking of elongated structures using statistical snakes. In *Proceedings of the CVPR*, pages 157–162, Hilton Head Island.

Xie, J. and Heng, P. A. (2005). Shape modeling using automatic landmarking. *Lecture Notes in Computer Science*, 3750:709–716.

Yushkevich, P., Fletcher, P. T., Joshi, S., Thall, A., and Pizer, S. (2003). Continuous medial representations for geometric object modeling in 2d and 3d. *Image and Vision Computing*, 21(1):17–28.